Sandwich-like heterostructured nanomaterials immobilized laccase for the degradation of phenolic pollutants and boosted enzyme stability

Li, Mengyu; Bai, Yahan; Zhuang, Wei; Liu, Jinle; Wang, Zhi; Rao, Yuan; Li, Mengran; Ying, Hanjie; Ouyang, Pingkai

DOI
10.1016/j.colsurfa.2022.130820

Publication date
2023

Document Version
Final published version

Published in
Colloids and Surfaces A: Physicochemical and Engineering Aspects

Citation (APA)
Li, M., Bai, Y., Zhuang, W., Liu, J., Wang, Z., Rao, Y., Li, M., Ying, H., & Ouyang, P. (2023). Sandwich-like heterostructured nanomaterials immobilized laccase for the degradation of phenolic pollutants and boosted enzyme stability. *Colloids and Surfaces A: Physicochemical and Engineering Aspects*, *660*, Article 130820. https://doi.org/10.1016/j.colsurfa.2022.130820

Colloids and Surfaces A: Physicochemical and Engineering Aspects 660 (2023) 130820

Contents lists available at ScienceDirect

Colloids and Surfaces A: Physicochemical and Engineering Aspects

journal homepage: www.elsevier.com/locate/colsurfa

Sandwich-like heterostructured nanomaterials immobilized laccase for the degradation of phenolic pollutants and boosted enzyme stability

Mengyu Li [a], Yahan Bai [a], Wei Zhuang [a,b,*], Jinle Liu [a], Zhi Wang [a], Yuan Rao [a], Mengran Li [c], Hanjie Ying [b], Pingkai Ouyang [b]

[a] School of Chemical Engineering, Zhengzhou University, Zhengzhou 450001, China
[b] College of Biotechnology and Pharmaceutical Engineering, State Key Laboratory of Materials-Oriented Chemical Engineering, National Engineering Technique Research Center for Biotechnology, Nanjing Tech University, No. 30, Puzhu South Road, Nanjing 211816, China
[c] Materials for Energy Conversion and Storage (MECS), Department of Chemical Engineering, the Delft University of Technology, van der Maasweg 9, Delft 2629 HZ, the Netherlands

GRAPHICAL ABSTRACT

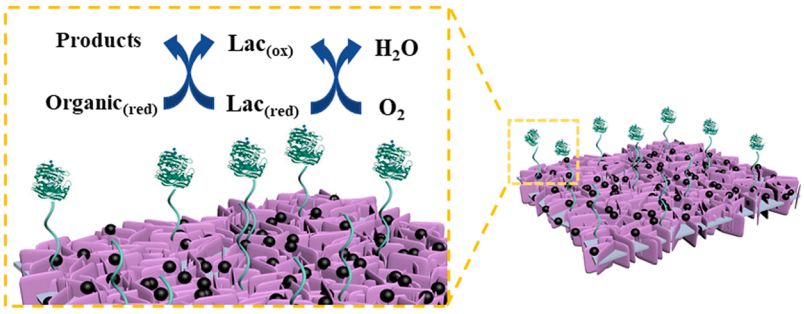

ARTICLE INFO

Keywords:
2D nanomaterials
Heterogeneous assembly
Immobilized laccase
Simulated industrial wastewater

ABSTRACT

A novel magnetic 2D/2D heterogeneous structure MXene@NiFe-LDH@Fe_3O_4 was prepared for immobilization of laccase. In this work, two-dimensional MXene nanosheets with abundant surface functional groups were heterogeneously assembled with layered double hydroxide (LDH) by in situ co-precipitation method, and magnetic nanoparticle Fe_3O_4 with excellent biocompatibility and rapid separation of materials and substrates was introduced subsequently, and then silane coupling agent was coated on the surface of MXene@NiFe-LDH@Fe_3O_4. The functionalized MXene@NiFe-LDH@Fe_3O_4 was employed as a carrier to immobilize laccase from *Trametes-Versicolor*. The enzyme loading of the nanocomposite material is as high as 167.9 mg/g. Compared with free enzymes, the immobilized laccase showed a notable improvement in stability in a wider range of pHs (2.0–8.0), temperatures (25–60 °C), and organic solvent concentration (1–5 M). The reusability study suggested that after 7 cycles of repeated catalysis, the degradation efficiency could reach 55.5% for 2,4-dichlorophenol, 92.1% for bisphenol A and70.9% for pyrocatechol. The results provide a new carrier preparation strategy for the efficient immobilization of laccase.

* Corresponding author at: School of Chemical Engineering, Zhengzhou University, Zhengzhou 450001, China.
E-mail address: weizhuang@njtech.edu.cn (W. Zhuang).

https://doi.org/10.1016/j.colsurfa.2022.130820
Received 6 September 2022; Received in revised form 1 December 2022; Accepted 17 December 2022
Available online 22 December 2022

1. Introduction

Phenolic compounds are persistent organic pollutants widely existing in the water environment, mainly from petrochemical, paper making, pharmaceutical, paint, etc., with strong toxicity, difficult degradation, persistence and other characteristics[1]. Without effective removal, they will cause long-term harm to the water environment[2,3]. In recent decades, the treatment strategies of organic wastewater are mainly based on physical methods, advanced oxidation processes, and biological methods[1,4,5]. Among them, the physical method separates organic pollutants from wastewater based on physical processes, such as adsorption, extraction, and precipitation, which only involve the phase transfer of the pollutants without substantial degradation. The advanced oxidation process has the advantages of strong oxidation capacity and a wide application range[6]. However, continuous application of energy or chemicals is required during the treatment process[7]. Therefore, the high energy consumption and cost are inevitable shortcomings. The biological method has the advantages of environmental protection, low operating cost and high degradation efficiency, so it has attracted great attention of researchers globally in recent years[4,6,8].

Laccase is a single electron oxidoreductase containing copper[9]. In the presence of oxygen, four copper ions in laccase interact with free radicals from reactive substrates and synergically transfer electrons through the three-nucleus copper cluster center, thus catalyzing the oxidation of lignin, phenol, aromatic amine, chlorophenol, thiophenol, dyes, etc.[10,11]. It is a widely used environment-friendly enzyme catalyst[12]. However, water-soluble enzymes suffer from poor stability, susceptibility to inactivation, and difficulty in reuse[13]. Therefore, enzyme immobilization technology methods such as adsorption[14]、cross-linking[15] and embedding[16] have been introduced to overcome these limitations.

The selection of carriers is the key to the immobilization process[17], a series of nanomaterials of different sizes and shapes have been reported in the field of biotechnology as new types of immobilized enzyme carriers[18,19]. MXene is a two-dimensional layered material composed of transition metal carbides, nitrides or carbonitrides[20], which can be prepared by selectively etching the main group element A layer from the corresponding MAX phase (A = Al, Si, Ge and other main group elements)[21], with large surface area, hydrophilicity, tunable conductivity and abundant surface functional groups (-OH, = O, -F)[22]. However, due to Van der Waals forces and interlayer π-π interactions [23], MXene as a carrier exhibits a strong tendency to agglomerate, resulting in stacking of nanosheets, hindering mass transfer and masking active sites[24].

Combining two-dimensional materials with zero-dimensional nanoparticles, one-dimensional nanowires or two-dimensional nanosheets to reasonably construct nanocomposite microstructures can effectively improve the stacking problem of nanosheets[25]. Layered Double Hydroxides (LDHs) are typical layered materials, which have attracted attention from the fields of water environmental treatment and electrochemical energy storage in recent years due to its unique layered structure and excellent exchangability of metal ions and interlayer anions on the laminates[26,27], its highly tunable 2D interlayer channel, can significantly improve the intercalation rate of biomolecules[28]. Compared with 2D MXene nanosheets, the 2D/2D heterogeneous structure of MXene@LDH provides superior specific surface area, adsorption sites and biocompatibility while improving the self-stacking of nanosheets. However, the nanomaterials currently used for laccase immobilization are usually in powder form, which is difficult to recover in practical applications. The deposition of magnetic particles on the surface of MXene@LDH can impart magnetically responsive properties to the composites and achieve rapid separation from the aqueous phase under the action of an external magnetic field, making them excellent carriers for enzyme immobilization[29].

In this study, we prepared MXene@NiFe-LDH nanocomposites using a chemical co-precipitation method to improve the self-stacking of nanosheets while increasing the specific surface area of the material. Magnetic nanoparticles were introduced to facilitate the rapid separation of materials and substrates, the synthesized magnetic composite MXene@NiFe-LDH@Fe_3O_4 was used as an immobilized enzyme carrier. The surface of the composites was modified with (3-Aminopropyl)triethoxysilane (APTES) to increase the loading of laccase, thus improving the overall catalytic efficiency. The immobilization conditions, enzymatic properties and applicability of immobilized enzymes in degrading organic pollutants (2,4-DCP, BPA, pyrocatechol) were also investigated.

2. Materials and methods

2.1. Materials

Laccase (E.C. 1.10.3.2) from Trametes versicolor was purchased from Sigma-Aldrich (Shanghai, China). Sodium dihydngen phoshate anhydrous (Na_2HPO_4), citric acid monohydrate, glutaraldehyde (50%), lithium fluoride (LiF), urea, (3-Aminopropyl) trimethoxysilane (APTES), 2,2′-azinobis(3-ethylbenzthiazoline-6-sulfonate) (ABTS), 1-Methyl-2-pyrrolidinone (NMP), ferric chloride hexahydrate ($FeCl_3{\cdot}6\ H_2O$), ferrous chloride tetrahydrate ($FeCl_2{\cdot}4\ H_2O$), ferric nitrate nonahydrate ($Fe(NO_3)_3{\cdot}9\ H_2O$), nickel nitrate hexahydrate ($Ni(NO_3)_2{\cdot}6\ H_2O$), $NH_3{\cdot}H_2O$ (28–30%), sodium hydroxide (NaOH), 2,4-dichlorophenol (2,4-DCP, purity ≥ 98%), bisphenol A (BPA, purity ≥ 99.0%) and pyrocatechol (purity ≥ 99.5%) were purchased from Aladdin (Shanghai, China). Ti_3AlC_2 (MAX, 200mesh) was obtained from Macklin (Shanghai, China). Hydrochloric acid (HCl) was supported by Sinopharm Chemical Reagent Co., Ltd.

2.2. Synthesis of MXene@NiFe-LDH nanohybrid

$Ti_3C_2T_X$-MXene nanosheets were prepared according to the reported method[24]. Firstly, the LiF (1.8 g) was dispersed in HCl (20 mL) and magnetically stirred for 10 min, Ti_3AlC_2 (1 g) was gradually added into the etching solution and continuously stirred for 24 h at 35 °C. Subsequently, the resulting suspension was washed with deionized water several times until the pH of the liquid became neutral. After that, the obtained intermediate product was further dispersed in deionized water, and the mixture was sonicated in ice-water bath for 2 h. Finally, by centrifuging at 4000 rpm for 30 min, the supernatant was poured to obtain a black $Ti_3C_2T_X$-MXene colloidal solution with a concentration of 5.88 mg/mL.

The obtained $Ti_3C_2T_X$-MXene colloidal solution (8.5 mL) was dispersed in 30 mL N-methyl-pyrrolidone and sonication for 10 min, followed by the addition of a mixed metal salt precursor consisting of Ni $(NO_3)_2{\cdot}6\ H_2O$ (3 mM), $Fe(NO_3)_3{\cdot}9\ H_2O$ (1 mM) and urea (12 mM). After stirring for 30 min, the solution was subjected to reflux at 100 °C for 5 h. Afterwards, the $Ti_3C_2T_X$ loaded with NiFe-LDH (MXene@NiFe-LDH, abbreviated as ML) was harvested and washed with deionized water and ethanol for several times before drying in freeze dryer.

Fe_3O_4 nanoparticles (IONPs) was in situ co-deposited on the surface of ML. Briefly, the mixed metal salt precursors containing $FeCl_3{\cdot}6\ H_2O$ (2 mM) and $FeCl_2{\cdot}4\ H_2O$ (1 mM) were dissolved in 50 mL degassed ultrapure water, 0.5 g ML powder was added after magnetic stirring for 10 min, then the pH of suspension above was adjusted to 10 with $NH_3{\cdot}H_2O$, and the reaction was stirred for 1 h under the protection of N_2 at 80 °C. Afterwards, the product was washed several times with deionized water until the pH value of the liquid was neutral. After freeze-drying, MXene@LDH@Fe_3O_4 (abbreviated as MLF) powder was obtained.

2.3. Functionalization of MLF

APTES was used to modify the surface of the composite material. Normally, 100 mg of MLF powder is dispersed in 100 mL of 50% ethanol aqueous solution and sonicated for 30 min. Then add 0.5 mL APTES and stir at room temperature for 10 min, then stir for 10 h under the

protection of nitrogen at 65 °C. After the reaction, the precipitate was washed with ethanol and deionized water to remove unbound APTES, and the MXene@LDH@Fe_3O_4-NH_2 (abbreviated as MLF-NH_2) was freeze-dried and stored at 4 °C for further use.

2.4. Characterization

The morphology and structure of $Ti_3C_2T_X$-MXene, ML and MLF were measured by scanning electron microscopy (SEM, Helios G4 CX) and transmission electron microscopy (TEM, JEM-1400Flash) equipped with energy dispersive spectrometer (EDS). The thickness of the $Ti_3C_2T_X$-MXene nanosheets was measured by atomic force microscope (Dmension fastscan, Bruker). The automatic specific surface and pore size distribution analyzer was used to evaluate the specific surface area of the sample (BET-Autosorb-iQA3200–4). The Fourier transform infrared spectroscopy (FTIR, Perkin Elmer-Spectrum 100) was used to investigate the surface functionalities of the samples. The structure and phase characteristics of the samples were characterized by X-ray diffraction (XRD, Bruker D8 Advance). The change of the composition and chemical states was characterized by an X-ray photoelectron spectroscopy (XPS, Thermo ESCALAB-250xi). The distribution of enzyme molecules which labeled by fluorescein isothiocyanate (FITC) was investigated using confocal laser scanning microscopy (CLSM, TCS SP5II, Leica). The vibrating sample magnetometer (VSM, Quantum-MPMS3) was used to examine the magnetic properties of the carriers. Ultraviolet-visible spectroscopy system (UV–vis, Agilent Cary 60) was used to test the peroxidase-like performance of the composite material, the loading amount of laccase, and the activity of free and immobilized laccase. The Zeta potential analyzer (Mastersizer 3000, Malvern) was used to assess the number of charges and electrostatic interactions on the nanosheets surface.

2.5. Immobilization of laccase on MLF-NH_2

The MLF-NH_2 nanocomposites were first dispersed in citric acid-dibasic sodium phosphate solution (100 mM, pH 4.0) to form a 5 mg/mL aqueous suspension. The laccase was also dissolved in a citric acid-dibasic sodium phosphate solution to form a 1 mg/mL buffered laccase solution. The immobilization was carried out by mixing 1.0 mL MLF-NH_2 disperse solution and desired amount of laccase and then incubating at 4 °C with shaking at 180 rpm. We separated the carrier with a magnet, collected the supernatant and washing liquid, collected the unreacted laccase. The amount of immobilized laccase was calculated using the Bradford assay method. The MLF-NH_2 loaded with laccase (MLF-NH_2-laccase, abbreviated as MLF-lac) was stored at 4 °C until the using time.

2.6. Laccase activity assay

Spectrophotometric determination of laccase activity was carried out by measuring the oxidation of ABTS rate according to the methods reported in the previous work[30]. Briefly, the reaction system containing an aliquot of free laccase, MLF-lac (5 mg) and ABTS solution (0.5 mM, 3 mL) prepared by citric acid-dibasic sodium phosphate buffer solution (100 mM , pH 4.0) was allowed to react for 3 min at 25 °C. The supernatant was filtered with a 0.22 μm filter, and the absorbance was measured at 420 nm using a UV-Vis spectrometer. One unit of the activity (U) was defined as the amount of laccase required to catalyze the oxidation of 1 μmol ABTS within one minute, the immobilization rate is calculated as follows[31].

$$\text{Expressed activity}(\text{U/g biocatalyst}) = A \times 10^6 \times V_t/(\varepsilon \times t \times m_1) \quad (1)$$

$$\text{Specific activity } (\text{U/g protein}) = A \times 10^6 \times V_t/(\varepsilon \times t \times m_2) \quad (2)$$

Where A is the absorbance of $ABTS^{2+}$ at 420 nm; Vt is the total volume of reaction system (L); ε is the molar extinction coefficient of $ABTS^{2+}$ (36,000 M^{-1} cm^{-1}); t is the reaction time (min); m_1 and m_2 are the amount of MLF-lac (g) and protein content of MLF-lac (g), respectively.

2.7. Optimization of immobilization conditions

The MLF-NH_2 carrier activated by different mass fractions (0% ~3.0%) of glutaraldehyde solution was used for the immobilization of laccase after reacting in a shaker at 25 °C for 2 h. To test the relative activity of the immobilized enzyme, the data with the highest activity was defined as 100%, and calculate the enzyme loading.

The effects of pH on the activities of MLF-lac were studied in a citric acid-disodium phosphate buffer with different pH values (2.0–9.0) at 25 °C. The relative activity at 40 °C was used as the control (100%) to calculate and compare the activity of MLF-lac, then calculate the enzyme loading.

The effect of temperature on the activities of MLF-lac was examined in a citric acid-disodium phosphate buffer at 20–80 °C for 30 min at constant pH of 4.0. The relative activity at pH 4.0 was used as the control (100%), and the remained activity of laccase was analyzed under the standard conditions above, then calculate the enzyme loading.

2.8. Stability of free and immobilized laccase

To investigate the thermal stability, free and immobilized laccase were cultured in 60 °C water for a period of time and the activity was measured every hour. The enzymatic activity without incubation was taken as the control (100%) to study the remaining activity (%) of free and immobilized laccase.

Organic solvent resistance was determined by incubating free and immobilized laccase in a series of concentrations of urea solution for 30 min. The activity was measured under the optimal conditions mentioned above, and the initial activity was defined as 100%.

Storage stabilities of free and immobilized laccase were assessed by measuring the remaining activity after being stored at 4 °C for one month, and the laccase activity was determined every five days. The laccase activity without incubation was taken as the control (100%), the residual activity was calculated and compared according to the method described above.

2.9. Reusability of immobilized laccase

The reusability was measured by evaluating the activity of the immobilized laccase activity after each cycle of removing the phenolic mixture (containing 0.5 mM ABTS) using MLF-lac (30 °C, pH 4.0). Further, the catalyst was washed several times with ultra-pure water after each cycle. The initial laccase activity was defined as the control (100%).

2.10. Removal of phenols

Immobilized laccase or an equal amount of laccase was added to 10 mL of 2,4-DCP (10 mg/L), BPA (10 mg/L) or pyrocatechol (10 mg/L) in an aqueous solution with ABTS (0.5 mM), which serve as a mediator substance[32]. The degradation of phenols took place in a shaker at 30 °C and 180 rpm for 12 h, the suspension was filtrated out with a 0.22 μm filter after degradation. The degradation degree was determined based on high-performance liquid chromatography with a C18 reversed-phase column (Agilent , 150 mm × 4.6 mm, 5 μm particles). Detection conditions of 2,4-DCP: mobile phase 70% methanol solution ; detection wavelength: 290 nm; column temperature : 35 °C; flow rate: 0.8 mL/min; time: 10 min. Detection conditions of BPA: mobile phase A (ACN): B (H_2O: THF: phosphoric =1:0.01:0.002 (v:v:v))= 1:1 ; detection wavelength: 214 nm; column temperature : 35 °C; flow rate: 0.8 mL/min; time: 10 min. Detection conditions of pyrocatechol: mobile phase 50% methanol solution ; detection wavelength: 280 nm; column

temperature : 35 °C; flow rate: 0.8 mL/min; time: 10 min. The degradation efficiency was calculated using the formula below[33]:

$$\text{Removal efficiency } (\%) = (C_o - C_f)/C_o \times 100\% \quad (3)$$

Where C_o and C_f represent the initial and the residual concentration of phenols after the enzyme treatment, respectively.

3. Results and discussion

Fig. 1 illustrates the synthesis route of nanocomposites for laccase immobilization and its application for organic phenols. Firstly , we obtained single few-layer nanosheets $Ti_3C_2T_X$-MXene by etching the Al layers from Ti_3AlC_2 MAX phase and dispersed it in water. Thus, urea and metal salts were added to the colloidal solution, urea hydrolysis caused the precipitation and crystallization of metal salts to achieve anisotropic growth of NiFe-LDH on the surface of MXene nanosheets, which significantly improve the specific surface area. We then deposited Fe_3O_4 nanoparticles on the surface of the synthesized nanocomposite to confer magnetic properties and facilitate separation. APTES then modified the surface of the composites by hydrolysis reaction, and the functional group of glutaraldehyde covalently attached the enzyme molecule to the surface of the carrier for the immobilization of the enzyme.

3.1. Synthesis and characterization

The nanomaterials from each synthesis stage are monitored by the scanning electron microscope and transmission electron microscope (Fig. 2). The exfoliated $Ti_3C_2T_x$-MXene nanosheets show a typical two-dimensional layered structure with a lateral size of 5–8 μm (Fig. 2a). The bending and wrinkles of the nanosheets indicate a high degree of flexibility. The AFM image shows that the peeled nanosheets have a flat surface and a thickness of about 2.5 nm (Fig. S1). Pure LDH behaves as a nanosphere structure with a diameter size of 1.5–2 μm (Fig. 2b). The ML nanohybrid shows a 2D/2D heterostructure, where NiFe-LDH grew in situ and was evenly distributed at the surface of a single layer of $Ti_3C_2T_x$-MXene (Fig. 2c). Obviously, ML provides a larger substrate contact area and more active sites than the $Ti_3C_2T_x$-MXene, which could benefit the charge transfer during the catalytic reaction. Magnetic nanoparticles Fe_3O_4 with a particle size of about 30 nm in the MLF are attached to the ML surface (Fig. 2d). TEM further confirmed the sheet structure of $Ti_3C_2T_x$-MXene and the successful assembly of the composite materials (Fig. 2g, h). The elemental analysis of the nanoparticles using EDS confirmed the presence and uniform distribution of C, Fe, Ni, Ti and O atoms (Fig. 2i-n) in ML.

The N_2 adsorption/desorption analysis further demonstrated that the heterogeneous assembly of $Ti_3C_2T_X$-MXene with NiFe-LDH can effectively increase the specific surface area of the composites. ML and MLF show a type IV adsorption isotherm with H3-type hysteresis loop (Fig. 3). The BET specific surface area and pore data are listed in Table 1, proving the existence of the mesoporous structure. It can be speculated that the longitudinal alignment of NiFe-LDH on the surface of $Ti_3C_2T_X$-MXene is the main source of mesopores, which is proved by the BET and pore volume data. After loading NiFe-LDH on the surface of $Ti_3C_2T_X$-MXene, we noted that the specific surface area increased from 1.8 m^2/g to 123.3 m^2/g, and the pore volume also increased by about 40 folds. Although the assembly of magnetic nanoparticles decreased the specific surface area of ML to 114.3 m^2/g, it can still be demonstrated that the NiFe-LDH can creat more abundant active sites.

The crystal structures of all nanomaterials were examined by XRD. As shown in Fig. 4a, the (002) at the center position of 7.0° is a characteristic peak of $Ti_3C_2T_X$-MXene, the diffraction peaks including (003), (006) and (009) are the characteristic peaks of NiFe-LDH crystal structure, in line with previous reports[34,35]. In the nanocomposite ML, the (002) characteristic peak from $Ti_3C_2T_X$-MXene can be clearly found, but the characteristic XRD peak position is shifted from the original 7° to a lower angle at 5.6°, it is indicated that the doping of NiFe-LDH increases the interlayer spacing between $Ti_3C_2T_X$-MXene nanosheets. XRD results confirm the successful combination of two materials. The characteristic peaks of NiFe-LDH are discernable in the MLF, but the (002) diffraction peak of $Ti_3C_2T_x$-MXene is weak and overlapped. MLF had the same crystalline characteristic peaks of the ML, which is an indication that the crystal structure was completely maintained. However, the intensity of the MLF diffraction peaks is weak, indicating a low degree of crystallization.

The FTIR spectra of MLF and MLF-NH_2 are shown in Fig. 4b. The absorption peak at 3350 cm^{-1} is attributed to the stretching vibration of

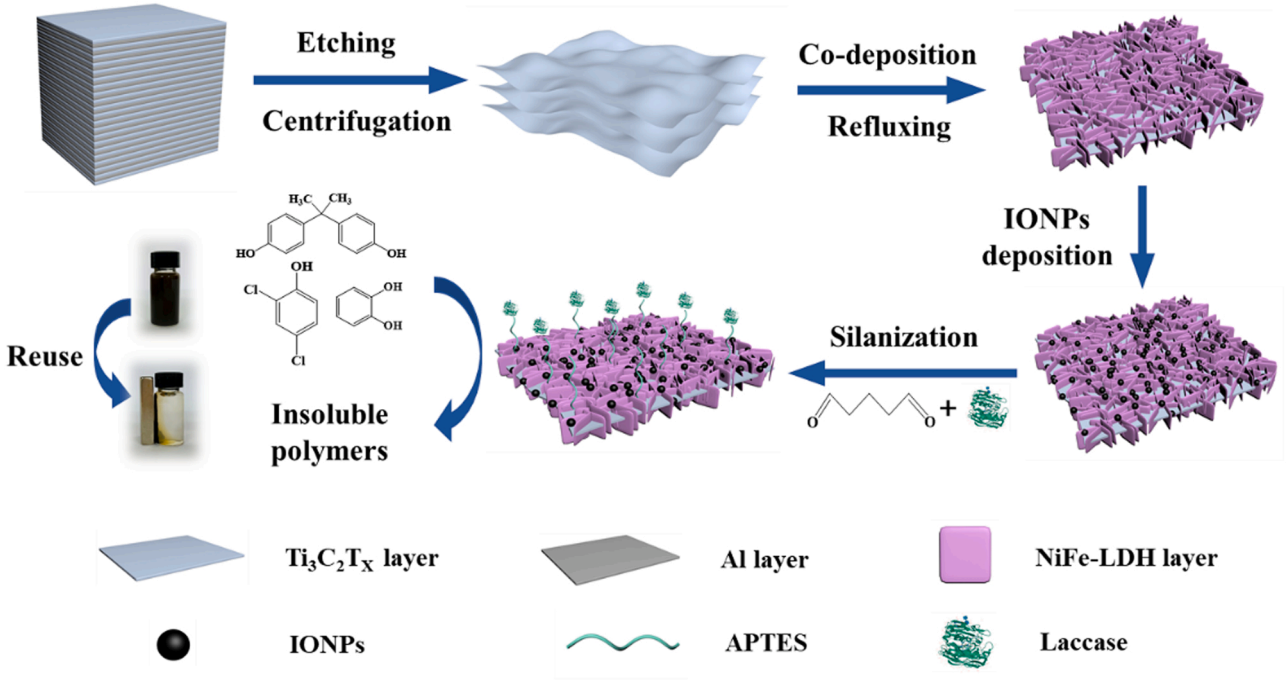

Fig. 1. Schematic graphic of the preparation of the immobilized laccase and degradation of organic phenols.

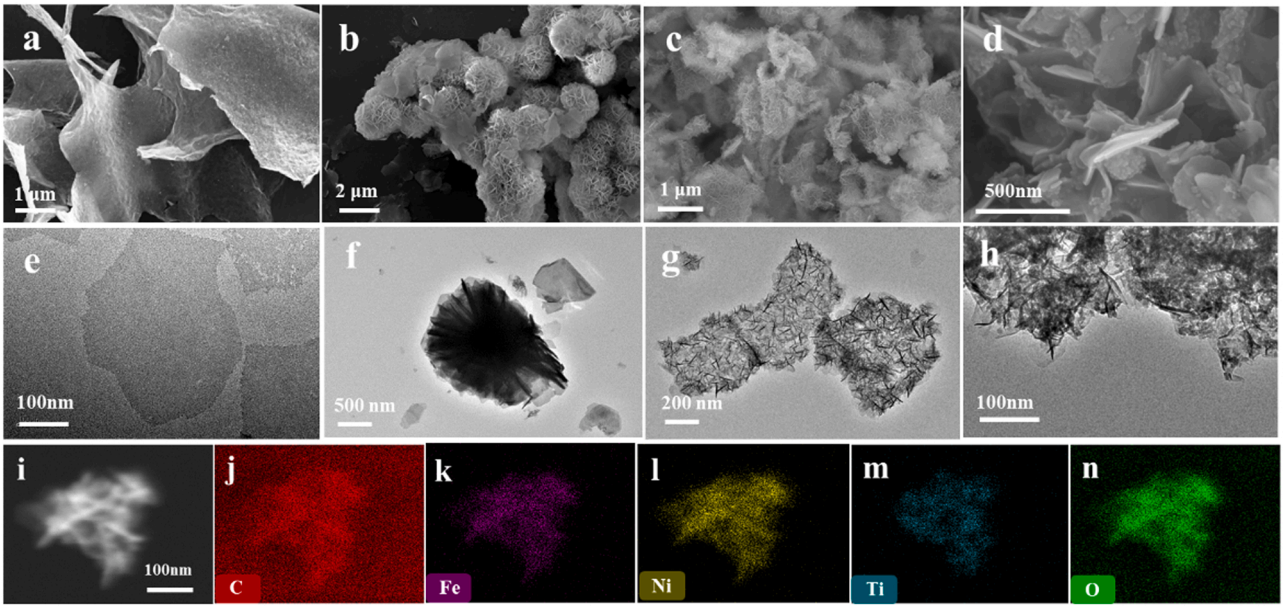

Fig. 2. SEM images of (a) $Ti_3C_2T_x$-MXene, (b) pure NiFe-LDH, (c) ML and (d) MLF nanomaterials; TEM images of (e) $Ti_3C_2T_x$-MXene, (f) pure NiFe-LDH, (g) ML and (h) MLF nanomaterials; (i) TEM dark field scanning and corresponding element mapping showing the uniform distribution of (j) C, (k) Fe, (l) Ni, (m) Ti, (n) O elements in the ML.

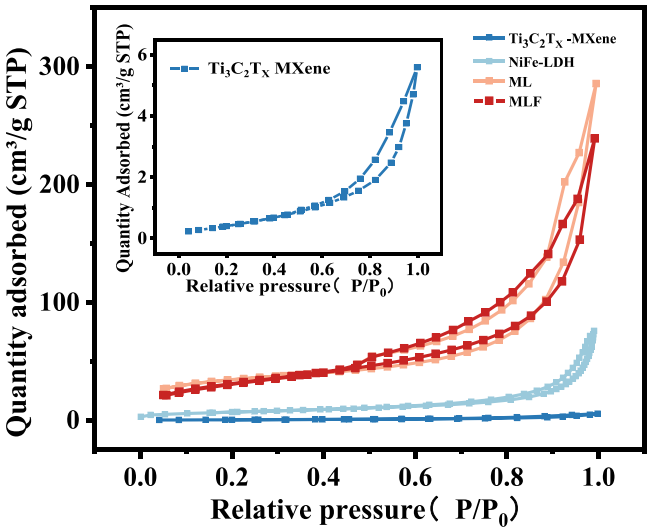

Fig. 3. N_2 adsorption-desorption isotherms of $Ti_3C_2T_x$-MXene, NiFe-LDH, ML and MLF nanocomposites.

Table 1
Pore characteristics for $Ti_3C_2T_x$-MXene, NiFe-LDH, ML and MLF.

Materials	BET Surface Area (m^2/g)	V_{BJH}/ (cm^3/g)		D_{BJH}/ (nm)	
		Adsorption	Desorption	Adsorption	Desorption
$Ti_3C_2T_x$-MXene	1.801	0.01	0.01	5.037	3.524
NiFe-LDH	25.333	0.121	0.121	12.758	10.709
ML	123.345	0.419	0.439	23.057	13.797
MLF	114.252	0.362	0.369	15.391	11.209

V_{BJH}——Adsorption and desorption cumulative volume of pores ;
D_{BJH}——Adsorption and desorption average pore size.

hydrophilic O-H. The peaks at 2973 cm^{-1} and 1193 cm^{-1} correspond to the stretching vibrations of C-F and C-O peaks, respectively. This data confirms the presence of rich functional groups on the MLF surface, consistent with the previous report[34]. In the spectral comparison of MLF and MLF-NH_2, the additional peaks in the spectrum of MLF-NH_2 unveil a strong absorption of Si-O (at 1066 cm^{-1})、N-H (at 1634 cm^{-1}) and C-N (at 1258 cm^{-1}) [36]. These peaks directly prove the successful modification of the silane coupling agent at the surface of the composite material.

The XPS survey spectra in Fig. 5a show that the main constituent elements of MLF nanocomposites are Ni, Fe, Ti, C and O. The presence of Si and N elements in the sample after surface functionalization with amino groups indicates that the silane coupling agent was successfully combined with the carrier. The Ti 2p high-resolution spectrum can be deconvoluted into four pairs of 2p3/2 and 2p1/2 doublets for Ti-C (453.7/461.0 eV), Ti^{2+} (467.2/462.8 eV), Ti^{3+} (458.8/464.1 eV) and Ti-O (459.3/456.1 eV) (Fig. 5b)[24], which are the Ti states in the $Ti_3C_2T_x$-MXene nanosheets. The Ni 2p spectrum shows two peaks of 2p 3/2 and 2p 1/2 and two satellite peaks at 861.77 eV and 879.76 eV (denoted as Sat.) (Fig. 5c)[37]. Two distinct peaks in the Fe 2p spectrum can be assigned to Fe 2p3/2 (711.1/713.2 eV) and Fe 2p1/2 (723.6/726.1) of Fe in Fe_3O_4 (Fig. 5d)[38]. The peaks of Si 2p can be associated with Si-O-C (101.70 eV) and Si-O-Si (102.89 eV) (Fig. 5e) [39], which further confirm the successful of amino-silane modification.

The modified amount of silane coupling agent and the relative mass of enzyme molecules on the surface of MLF composites can be estimated by thermal gravimetric analysis of MLF, MLF-NH_2, and MLF-Lac under programmed temperature conditions (Fig. 6a). The thermogravimetric loss curves of the three materials are shown in Fig. 6b. The MLF lost about 21.9 wt% mass during the whole heating process (15–800 °C). When the surface is coated with a silane coupling agent, MLF-NH_2 exhibits the same weight loss trend as MLF at below 350 °C, but an additional mass loss of about 3.0 wt% occurs between 350 and 600 °C, which is possibly a result of the thermal decomposition of APTES. Therefore, we can conclude that the silane coupling agent was successfully grafted on the MLF surface. The weight loss curve of MLF-Lac showed an additional mass difference of about 2.1% compared to MLF-NH_2, which was attributed to the immobilization of the laccase on the support surface and the decomposition of the crosslinker glutaraldehyde. Data

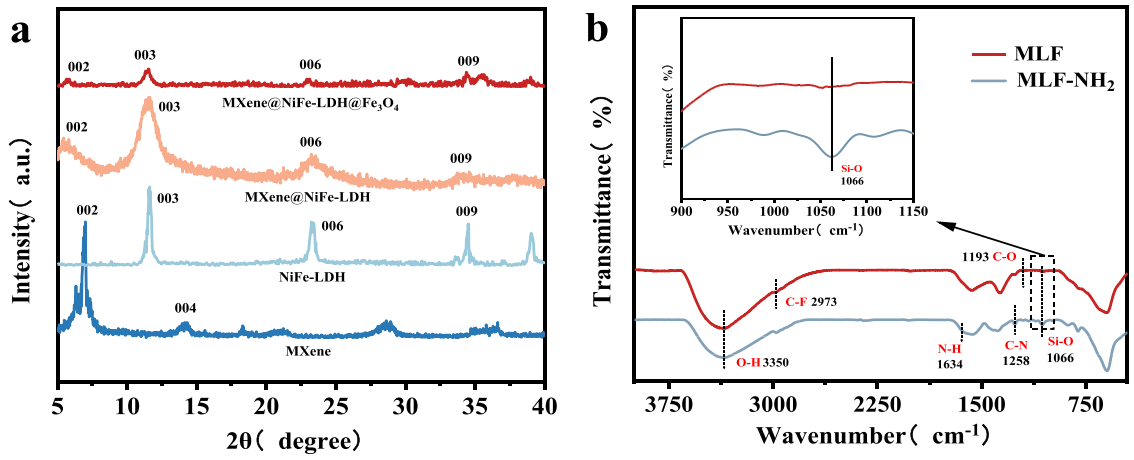

Fig. 4. (a) The XRD pattern of the NiFe-LDH, ML and MLF; (b) The FTIR spectrum of MLF and MLF-NH_2.

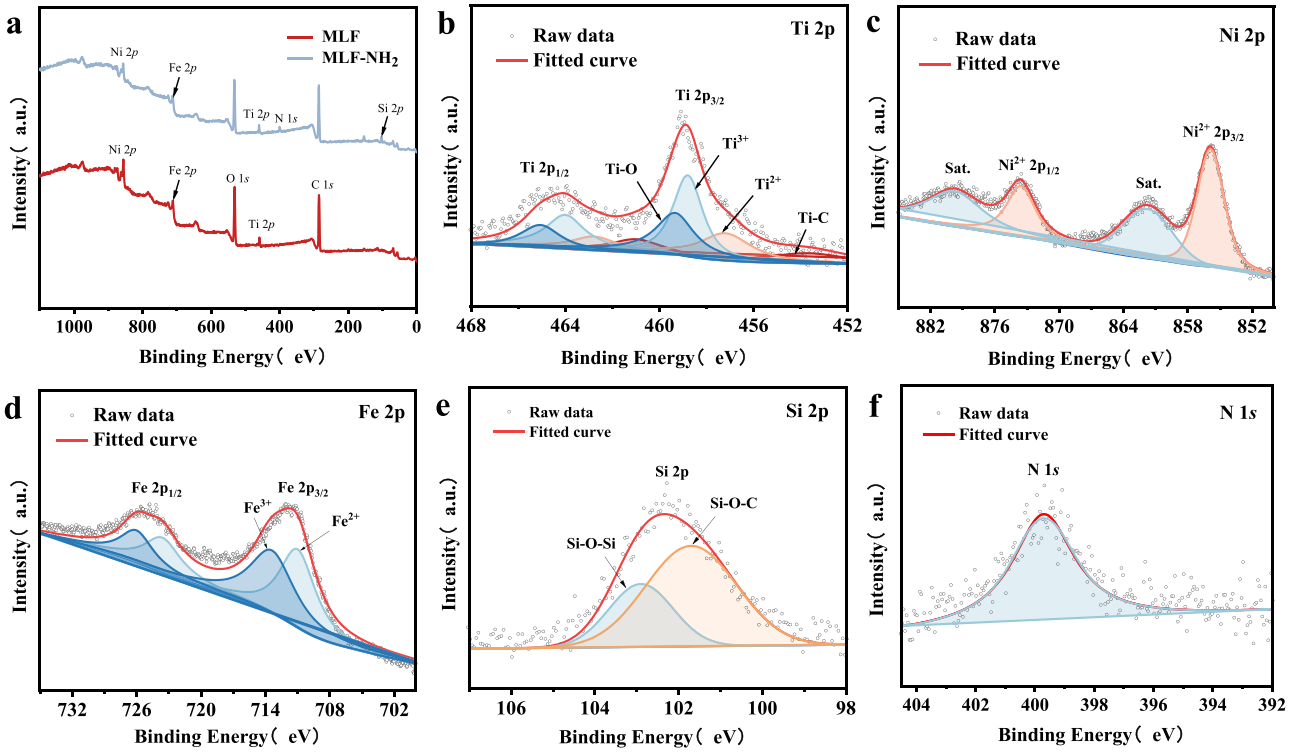

Fig. 5. The comparison of the XPS survey scan of MLF and MLF-NH_2 (a) and the high resolution XPS spectrum of (b) Ti 2p, (c) Ni 2p, (d) Fe 2p, (e) Si 2p and (f) N 1 s of MLF-NH_2.

analysis of TGA confirmed the successful preparation of immobilized laccase MLF-Lac. The surface potentials of the materials were further studied (Fig. S4). After APTES modification, the negative charge carried by the surface of MLF-NH_2 is enhanced, which further indicates the successful modification of APTES. Laccase is negatively charged when the substrate pH is greater than the isoelectric point, so there is an electrostatic attraction between MLF-NH_2 and laccase. Moreover, the immobilization of labeled enzymes on the surface of nanocomposites was visualized under CLSM. The observations were documented by labeling laccase. A clear green fluorescence can be observed in the image of MLF-Lac in Fig. S3, indicating that the laccase labeled by FITC stain is uniformly immobilized on the surface of the vector.

The magnetization of MLF, MLF-NH_2 and MLF-Lac were investigated by a vibrating sample magnetometer (Fig. 6b). It can be observed that MLF nanoparticles had a relative strong magnetism, approximately 23.1 emu/g. After functionalization of the MLF surface with amino groups, the MLF-NH_2 has a saturation magnetization of 16.3 emu/g. Such damped magnetization is likely a result of the coated silane coupling agent. After immobilizing the enzyme, we noted that a multi-layer coating was formed at the surface of MLF, which further reduced the magnetic properties of the material.As can be seen from the inset, although the saturation magnetization of the immobilized enzyme is 9.5 emu/g lower than that of MLF, the magnet could easily separate the nanocomposites from aqueous solution under the intervention of an external magnetic field, shows a compelling application prospect.

3.2. *Optimization of laccase immobilization*

Glutaraldehyde plays an important role in the immobilization of the enzyme as a bridge between the enzyme molecule and the carrier.

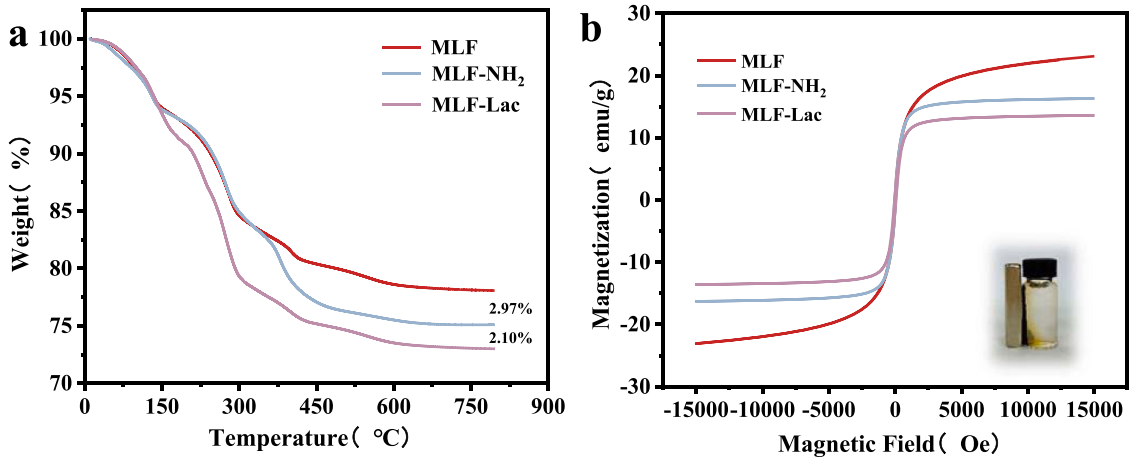

Fig. 6. (a) TGA curves of MLF, MLF-NH_2 and MLF-Lac; (b) Magnetic hysteresis loop of MLF, MLF-NH_2 and MLF-Lac.

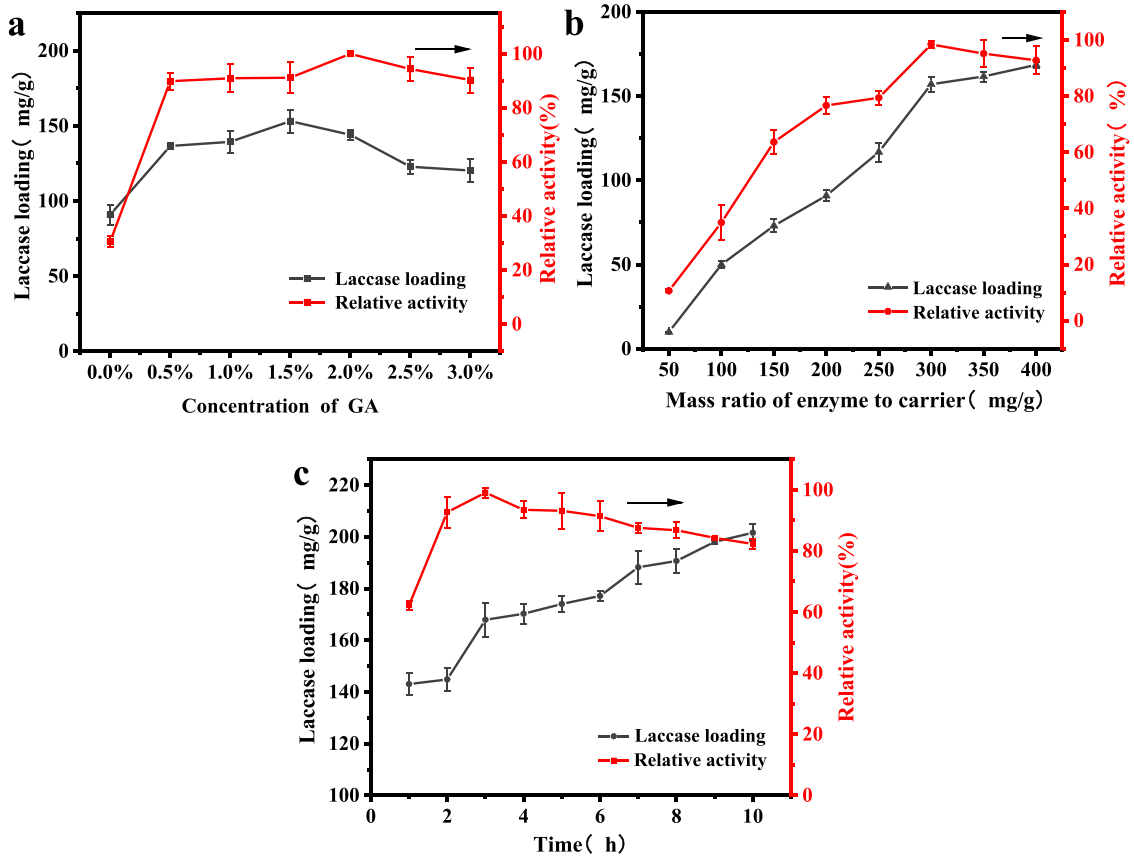

Fig. 7. Optimization of immobilized enzyme conditions: (a) glutaraldehyde concentration; (b) mass ratio of enzyme to carrier; (c) immobilization time.

Fig. 7a shows the relationship between glutaraldehyde concentration and enzyme loading and relative activity of immobilized enzyme. When the GA concentration is 0.0% (i.e., the immobilization method is adsorption), the relative activity of MLF-Lac is only 30.5%. With the increase of the mass fraction of glutaraldehyde, the enzyme loading and relative activity of the immobilized enzyme increased first and then decreased. This may be due to the fact that as the glutaraldehyde mass fraction increases, more enzyme molecules are covalently bound to the surface of MLF-NH_2 through the Schiff's base reaction to form amide bonds. When the concentration of glutaraldehyde reaches 2.0%, the relative activity of the immobilized enzyme reached its maximum value, at which time the enzyme loading was 144.1 mg/g. Continuing to increase the amount of glutaraldehyde, the excessive cross-linking agent produced a large intramolecular or intermolecular cross-linking with the amino groups of the enzyme, resulting in a decrease in the binding ability of the enzyme and carrier, while the tightly cross-linked enzyme aggregates might mask or change the original structure of the enzyme, leading to a decrease in relative enzyme activity. The results showed that the optimum concentration of glutaraldehyde was 2.0%.

The initial laccase concentration can influence the relative enzyme activity of MLF-Lac nanocomposites. As the content of laccase increases, as shown in Fig. 7a, the loading of laccase gradually increases. Consequently, the relative activity of the MLF-lac reaches the maximum when 300 mg of laccase was introduced. At this point, the enzyme load

reached 157.1 mg/g. However, the relative activity began to degrade with a further increase of laccase loading. The reason could be that the overcrowded laccase destabilizes its conformation, and thus blocks or deactivates some of the active centers. The relative activity of the immobilized laccase is enhanced with the immobilization time (Fig. 7b). However, the activity of the immobilized enzyme reached the maximum at 3 h of the immobilization time and began to drop thereafter. This trend could be a result of the long-term shaking that can cause denaturation of laccase in solution, or the overcrowded accumulation of laccase changes its stable conformation[40].

We can conclude that the optimal duration for laccase immobilization is 3 h with the loading efficiency of 167.9 mg/g. The immobilization efficiency and the relative enzyme activity as achieved in this work are superior to the reported data in the prior literature. As shown in Table 2, compared with the immobilized carriers reported in the literatures, MLF-NH_2 exhibited better performance. For the design of magnetic carriers, MLF-NH_2 in this work used a two-dimensional material as the main framework, which provided a broader space for the immobilization of enzyme molecules and substrate diffusion by coupling magnetic particles with two-dimensional nanomaterials. While other magnetic carriers regarded magnetic nanoparticles Fe_3O_4 as the main body for structural modification and surface modification, however, the particle size of Fe_3O_4 restricted the active surface of these carriers.

In the present work, the higher enzyme loading of MLF-NH_2 was mainly attributed to two reasons. Firstly, the porous mesh structure and high specific surface area formed by the coupling of $Ti_3C_2T_X$-MXene nanosheets with NiFe-LDH provided a wide space for laccase adsorption and maintenance of the three-dimensional conformation, while the larger reaction area increased the mass transfer area and reduced the adverse effect of substrate diffusion limitation on the enzyme molecules. Secondly, the coating of APTES provided a large amount of active amino groups, which provided a bioaffinity microenvironment for the immobilization and enzymatic reaction of laccase.

3.3. Enzymatic activity of free laccase and immobilized laccase on MLF-Laccase

3.3.1. Effect of pH and temperature on free and immobilized laccase

The pH and temperature serve as important roles in determining the enzyme activity. We found from Fig. 8a that immobilized laccase shows a much higher stability in a wider pH condition than the free laccase at room temperature. The free enzyme is at an optimal pH of 4.0, while the immobilized enzyme is at ~5, MLF-laccase shows an improvement of activity at pH > 4. This phenomenon can be well explained by the theory that the immobilized enzymes have a more stable conformation due to its multipoint attachment with their supporting materials, which have been well reported elsewhere[44]. The laccase is connected to the MLF through the bifunctional cross-linking reagent glutaraldehyde. Such feature reduces the molecular mobility of the enyzme. Additionally, the large carrier surface as obtained by MLF provides multiple attachment sites for laccase to maintain its conformation, enabling the enzyme to resist acid and alkaline adverse environments.

Fig. 8b compares the effect of temperatures on free and immobilized laccase activity and shows that the optimal temperature for both free and immobilized laccase are both 30 °C. Immobilized laccase sustained 60.02% of the peak activity when the temperature reached 60 °C, meanwhile the free laccase shows only 19.04% of the activity at the same temperature. Enzymes are easily denatured at high temperatures, which indicates that the secondary and tertiary structures of free enzyme molecules undergo irreversible changes at high temperatures. However, the temperature sensitivity of immobilized laccase is significantly lower than that of free laccase due to the beneficial effects of the carrier that stabilizes the conformation of the enzyme and its structure at high temperatures.

Table 2
Comparison of loading capacity and enzyme activity recovery rate of various composite materials immobilized enzymes.

Supporting	Bound enzyme (mg/g)	Activity retention (%)	References
Fe_3O_4-PDA	171	51.00	[32]
Fe_3O_4 @MoS_2 @PEI	120.00	90.00	[33]
PDA/HNTs	41.28	82.67	[41]
Fe_3O_4-NH_2-Cu^{2+}	76.03	42.74	[42]
Fe_3O_4 @SiO_2-chitosan	158	79.10	[43]
MLF-NH_2	167.91	76.92	This work

3.3.2. Stability of free and immobilized laccase

Denaturants can cause protein denaturation and therefore affect the practical application of laccase. Different concentrations of urea were prepared as denaturants to measure the organic solvent tolerance of free laccase and immobilized laccase. Fig. 8c shows the relationship between the relative activities of free laccase and immobilized laccase as a function of denaturant concentration. When the denaturant concentration increases, the relative activity of the enzyme is significantly reduced. Generally, however, the degree of degradation of the immobilized laccase is much lower than that of the free laccase. When the urea concentration is 1 mol·L^{-1}, the relative activity of is 81%, for the immobilized laccase, but is only 57% for the free laccase. Continuing to increase the urea concentration to 7 mol·L^{-1}, we noticed that the relative activity of the immobilized laccase still retains 20%, In contrast, free laccase, as common protein, completely lost its activity. Urea denatures proteins through destructing hydrophobic interaction by increasing the solubility of hydrophobic amino acids and therefore destroys the structure of protein[45].

Stability is a critical part of the research on the enzymatic properties of immobilized enzymes. Free and immobilized laccase were cultivated at 60 °C for 7 h to assess their thermal stability and the results were displayed in Fig. 8d. Owing to the destruction of the secondary and tertiary structures of the enzyme by the high temperatures, free laccase almost lost all its activity compared with its initial activity after 7 h. In contrast, the thermal stability of immobilized laccase was improved and retained 20% of activity after 7 h. It could be interpreted as the result of the combined action of various forces, such as hydrogen bonds, electrostatic force, and coordination bonds, which inhibited the stretch deformation of laccase molecules to maintain laccase activity[40].

3.4. Michaelis-Menten kinetics of free and immobilized laccase

The Michaelis constant K_m is the basic constant of enzyme kinetics [46]. It represents the concentration of the substrate when the enzyme reaction rate reaches half of the maximum reaction rate and reflect the affinity of the enzyme to the substrate[33]. The K_m and the maximum velocity of enzyme-catalyzed reaction (V_{max}) of free laccase and immobilized laccase were calculated using the Line weaver-Burk plots (Fig. 9). Free laccase presents an apparent K_m of 0.0758 mM and a maximum reaction rate V_{max} of 0.4889 mM/min. The immobilized enzyme MLF-lac presents an apparent K_m of 0.1401 mM and a maximum reaction rate V_{max} of 0.2122 mM/min. The Michaelis constant K_m of the immobilized enzyme is obviously higher than that of the free enzyme, indicating that the affinity of the immobilized enzyme to the substrate is smaller than free enzyme. This could be related to the steric hindrance of the immobilized carrier to the catalytic activity center of the enzyme. In addition, the two-way diffusion of the substrate and the reaction product is also restricted by steric hindrance, resulting in a decrease in the catalytic ability of the immobilized laccase[47].

3.5. Degradation of organic phenol by free and immobilized laccases

In this study, catechol, chlorophenols 2,4-dichlorophenol (2,4-DCP) and polycyclic aromatic hydrocarbons bisphenol A (BPA), which are

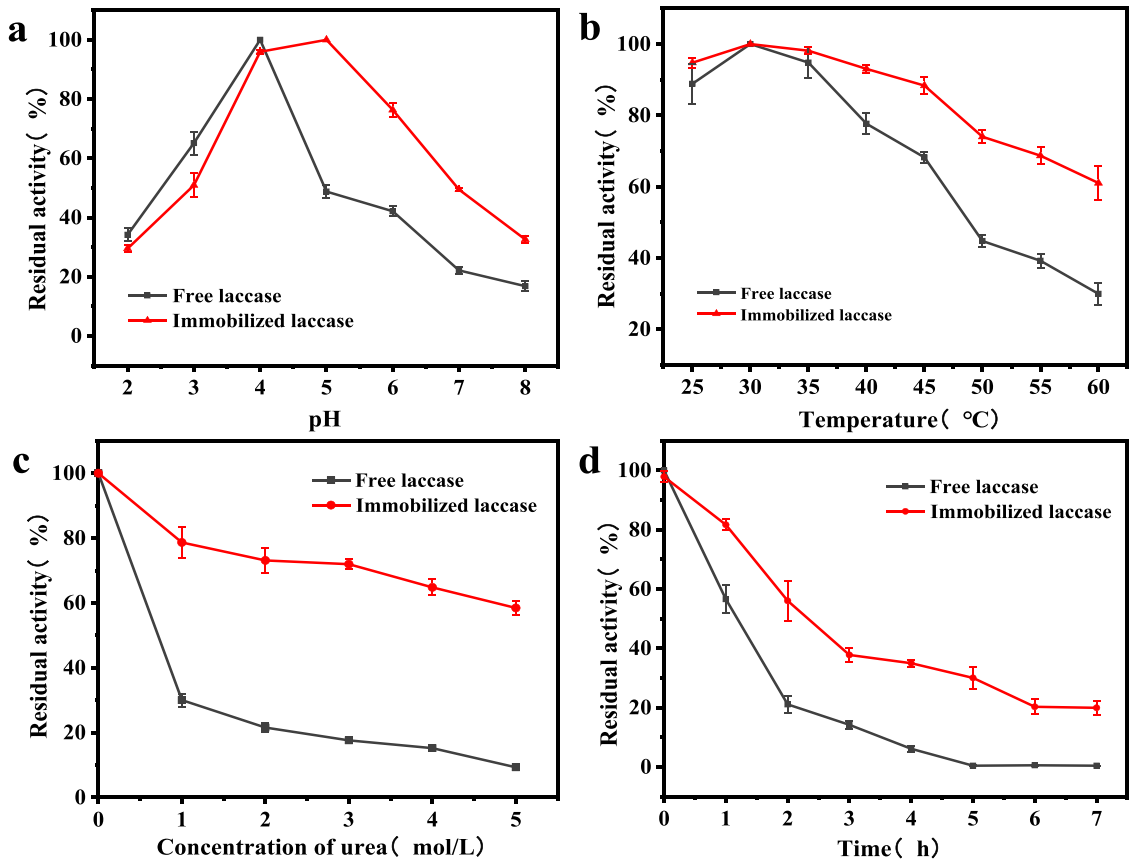

Fig. 8. Effect of (a) pH (b) temperature on the activity of the free and MLF-lac; (c) Effect of urea with different concentrations and (d) the thermal stability (at 60 °C) on the stability of the free and immobilized laccase.

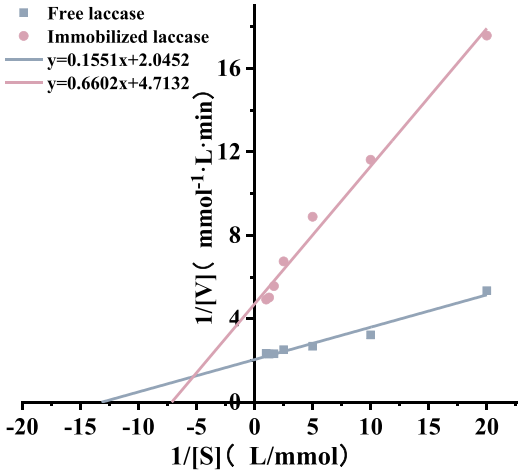

Fig. 9. The Lineweaver-Burk plots of free and immobilized laccase;.

common organic phenols in industrial wastewater, were selected as target substrates to evaluate the enzymatic activity. Laccase is usually used to study the removal of organic phenol in water on account of its unique advantages, especially avoiding secondary pollution[48]. In principle, the laccase is able to remove organic phenol by oxidizing it to form active radicals, which can polymerize the phenols to polymers that can be precipitated with low toxicity from water. Fig. 10a compared the removal efficiency of 2,4-DCP, BPA, and pyrocatechol in water by carrier MLF-NH_2, free laccase and MLF-lac at 25 °C. The removal efficiency of free laccase for 2,4-DCP, BPA, and pyrocatechol is 75.34%, 90.66% and 97.73%, respectively, while MLF-lac exhibits the removal efficiency of 93.94%, 95.76% and 100% for the three organic phenols, respectively.

The degradation rates of free enzymes and immobilized enzymes to three organic phenols in different reaction durations are shown in the Fig. 10b, c. High degradation rate were observed in both the initial 4 h. However, the removal efficiency of organic phenols by free and immobilized laccase gradually decreased in the following response period, which might be attributed to the decrease in the concentration of three organic phenols that available for the reactions.

Excellent reusability is essential for practical applications. To reduce the material cost, the magnetic immobilized enzyme can be separated by a magnet after the reaction and reused. From Fig. 10d-f, after seven repeated runs, approximately 55.49%, 92.11% 70.98% of removal efficiency could be retained for immobilized laccase according to 2,4-DCP, BPA and pyrocatechol, respectively. In addition to excellent catalytic performance, the catalytic material also needs to show excellent adsorption performance to pre-enrich organic matter locally near the surface of the catalyst for efficient phenol degradation. Therefore, we compared the changes in the adsorption capacity of the carrier for organic phenols during the repeated utilization process. MLF-NH_2 nanocomposite could also remove 21.41% 2,4-DCP, 44.98% BPA, 14.58% pyrocatechol only by surface adsorption. The decreased degradation efficiency of immobilized enzyme in the process of reusability likely due to (1) the congestion of reaction products which block the channels and hinder the access to substrates[32] and/or (2) the enzyme detachment and deactivation during constant mechanical stirring[49].

3.6. Comparison of the performance of some immobilized laccase

The comparison results of different organic compounds removal performance of laccase immobilized on various carriers are summarized

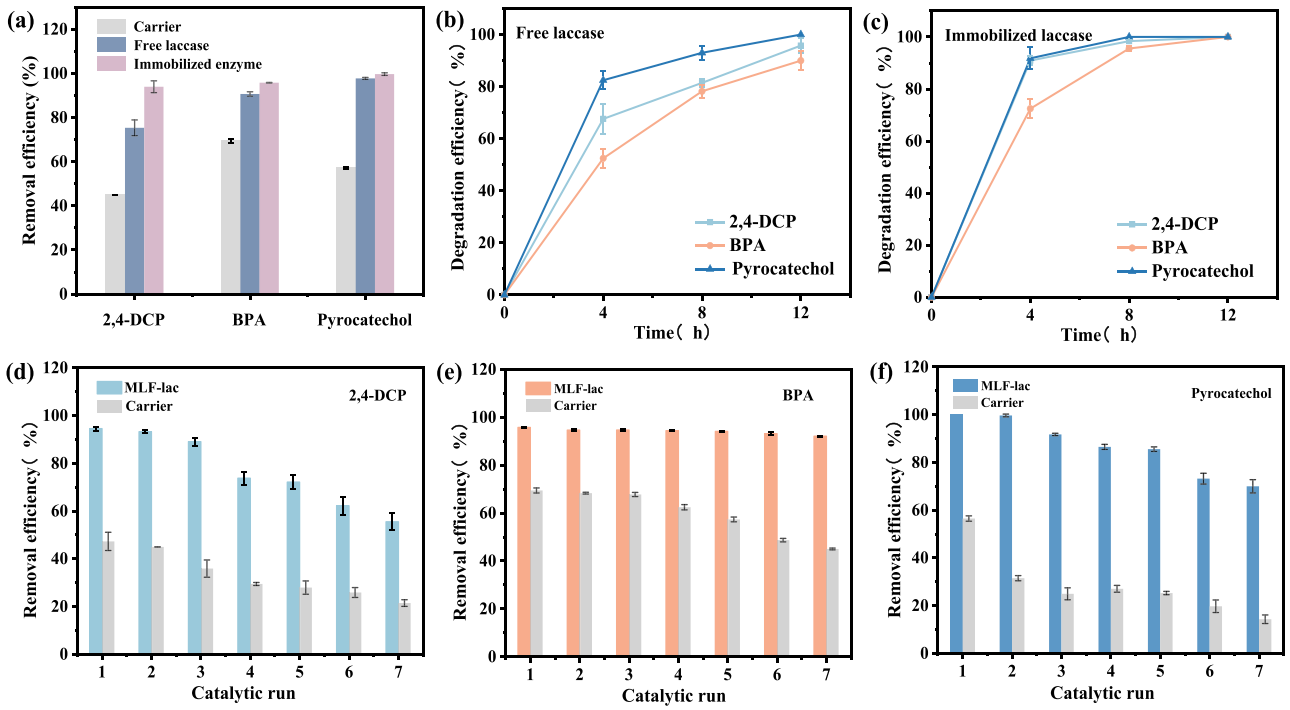

Fig. 10. (a) Removal efficiency of 2,4-DCP, BPA and pyrocatechol catalyzed by carrier, free laccase and immobilized laccase; Removal efficiency of 2,4-DCP, BPA and pyrocatechol catalyzed by (b) free laccase and (c) immobilized laccase in different time periods; Reusability of immobilized laccase and MLF nanocomposite in the removal of (d) 2,4-DCP, (e) BPA, (f) pyrocatechol. Experimental conditions: 2,4-DCP (10 mg/L), BPA (10 mg/L), Pyrocatechol (10 mg/L), pH7.0, 30 ℃, 10 mL, 12 h.

Table 3
Comparison of organic compounds removal performance of laccase immobilized on various carriers.

Laccase source	Immobilized enzyme	Substrate	Degradation (%)	References
Trametes versicolor	PP-co-pGMA-laccase	Crystal Violet (CV), Procion Green H 4 G (PG-H4G), Brilliant Blue G (BBG)	99%, 100%, 90%	[50]
Trametes versicolor	PS-co-DVB-g-P(CCMA)-laccase	Bisphenol A, Congo Red dye	89%, 100%	[51]
Trametes versicolor	p(MMA-EGMA-CCMA)-laccase	Methylene Blue dye, Carbaryl pesticide	63%, 71%	[52]
Trametes versicolor	p(HEMA-co-VC)-laccase	Cibacron Blue 3GA (CB3GA)	100%	[53]
Trametes versicolor	PET/ABTS@UiO-66(Zr)-NH_2-laccase	Crystal Violet (CV), Malachite Green (MG), Alizarin Green (AG), Methyl Orange (MO)	58.8%, 64.8%, 61.6%, 21.1%	[54]
Trametes versicolor	laccase-AS@BC/GMA-DA	2,4,5-trichlorophenol	98.3%	[55]

in Table 3. It is obvious from Table 3 that immobilized laccase has a very wide range of applications in the degradation of phenolic pollutants, polycyclic aromatic hydrocarbons and dyes. The ability of laccase to catalyze a variety of aromatic compounds makes it attractive for industrial applications.

4. Conclusions

To sum up, the novel MXene@NiFe-LDH@Fe_3O_4 nanocomposites were successfully prepared through the heterogeneous assembly of two-dimensional $Ti_3C_2T_X$-MXene nanosheets, layered double hydroxides (LDHs) and magnetic nanoparticles. Afterwards, covalently connected fixed laccase through interface modification. The results showed that the MXene@NiFe-LDH@Fe_3O_4 nanocomposites exhibited a larger specific surface area of 114.3 m^2/g, providing more attachment sites for the enzyme molecules. The coating of APTES provides reactive groups for nanocomposites, and laccase was successfully immobilized on their surfaces by cross-linking agents with a loading of 167.9 mg/g. The MLF-Lac showed better tolerance to acidic/alkaline acids, high temperature and organic solvents compared with free laccase, and excellent operation stability. Moreover, the degradation efficiency of MLF-Lac for 2,4-DCP, BPA, and pyrocatechol was 93.94%, 95.76% and 100% within 12 h, which was higher than that of free laccase. We expect that the nanoreactor with superparamagnetic properties can provide more ideas for the application of high-performance biocatalysts.

CRediT authorship contribution statement

Mengyu Li : Writing – original draft, Validation, Formal analysis, Visualization, Methodology. **Yahan Bai:** Data curation, Investigation. **Wei Zhuang** : Methodology, Writing – review & editing, Supervision, Resources, Funding acquisition. **Jinle Liu:** Project administration, Methodology. **Zhi Wang:** Resources, Data curation. **Yuan Rao:** Formal analysis, Data curation, Validation. **Mengran Li:** Investigation,

Visualization. **Hanjie Ying:** Funding acquisition, Resources. **Pingkai Ouyang:** Funding acquisition.

Declaration of Competing Interest

The authors declare that they have no known competing financial interests or personal relationships that could have appeared to influence the work reported in this paper.

Data Availability

Data will be made available on request.

Acknowledgment

This work was supported by grants from the National Key Research and Development Program of China (Grant No.: 2021YFC2102805, 2019YFD1101204), the National Natural Science Foundation of China (Grant No.: 21878142, 22008119, 22178170), Key Research and Development Plan of Jiangsu Province (Grant No.: BE2020712, BE2019001), the Six talent peaks project in Jiangsu Province (SWYY-016), the Jiangsu Synergetic Innovation Center for Advanced Bio-Manufacture, Jiangsu Natural Science Fund for Distinguished Young Scholars (Grant No.: BK20190035), and the Priority Academic Program Development of Jiangsu Higher Education Institutions (PAPD).

References

[1] V.I. Parvulescu, F. Epron, H. Garcia, et al., Recent progress and prospects in catalytic water treatment, Chem. Rev. 122 (3) (2022) 2981–3121.
[2] K.-H. Kim, S.-K. Ihm, Heterogeneous catalytic wet air oxidation of refractory organic pollutants in industrial wastewaters: a review, J. Hazard. Mater. 186 (1) (2011) 16–34.
[3] J. Zdarta, T. Jesionowski, M. Pinelo, et al., Free and immobilized biocatalysts for removing micropollutants from water and wastewater: Recent progress and challenges, Bioresour. Technol. 344 (2022), 126201.
[4] S. Ye, M. Yan, X. Tan, et al., Facile assembled biochar-based nanocomposite with improved graphitization for efficient photocatalytic activity driven by visible light, Appl. Catal. B: Environ. 250 (2019) 78–88.
[5] M. Patel, R. Kumar, K. Kishor, et al., Pharmaceuticals of emerging concern in aquatic systems: chemistry, occurrence, effects, and removal methods, Chem. Rev. 119 (6) (2019) 3510–3673.
[6] M. Coha, G. Farinelli, A. Tiraferri, et al., Advanced oxidation processes in the removal of organic substances from produced water: potential, configurations, and research needs, Chem. Eng. J. (2021) 414.
[7] A.K. Plappally, J.H. Lienhard, Energy requirements for water production, treatment, end use, reclamation, and disposal, Renew. Sustain. Energy Rev. 16 (7) (2012) 4818–4848.
[8] Z. Chen, S. Zhang, Y. Liu, et al., Synthesis and fabrication of g-C_3N_4-based materials and their application in elimination of pollutants, Sci. Total Environ. 731 (2020), 139054.
[9] J. Zdarta, A.S. Meyer, T. Jesionowski, et al., Multi-faceted strategy based on enzyme immobilization with reactant adsorption and membrane technology for biocatalytic removal of pollutants: a critical review, Biotechnol. Adv. 37 (7) (2019), 107401.
[10] A.A. Kadam, J. Jang, D.S. Lee, Supermagnetically tuned halloysite nanotubes functionalized with aminosilane for covalent laccase immobilization, ACS Appl. Mater. Interfaces 9 (18) (2017) 15492–15501.
[11] L. Munk, A.K. Sitarz, D.C. Kalyani, et al., Can laccases catalyze bond cleavage in lignin? Biotechnol. Adv. 33 (1) (2015) 13–24.
[12] J. Zdarta, L.N. Nguyen, K. Jankowska, et al., A contemporary review of enzymatic applications in the remediation of emerging estrogenic compounds, Crit. Rev. Environ. Sci. Technol. 52 (15) (2022) 2661–2690.
[13] T. Jesionowski, J. Zdarta, B. Krajewska, Enzyme immobilization by adsorption: a review, Adsorp. J. Int. Adsorp. Soc. 20 (5–6) (2014) 801–821.
[14] W. Zhou, W. Zhang, Y. Cai, Enzyme-enhanced adsorption of laccase immobilized graphene oxide for micro-pollutant removal, Sep. Purif. Technol. 294 (2022), 121178.
[15] L. Zhang, C. Han, P. Zhang, et al., Ultrafine platinum nanoparticles confined in a covalent organic framework for enhanced enzyme-mimetic and electrocatalytic performances, Nanoscale 13 (44) (2021) 18665–18676.
[16] Y. Feng, X. Cao, L. Zhang, et al., Defect engineering of enzyme-embedded metal-organic frameworks for smart cargo release, Chem. Eng. J. 439 (2022), 135736.
[17] J. Qu, S. Wei, Y. Liu, et al., Effective lead passivation in soil by bone char/CMC-stabilized FeS composite loading with phosphate-solubilizing bacteria, J. Hazard. Mater. (2022) 423.
[18] J. Zdarta, A.S. Meyer, T. Jesionowski, et al., Developments in support materials for immobilization of oxidoreductases: a comprehensive review, Adv. Colloid Interface Sci. 258 (2018) 1–20.
[19] J. Zdarta, A.S. Meyer, T. Jesionowski, et al., A general overview of support materials for enzyme immobilization: characteristics, properties, practical utility, Catalysts 8 (2) (2018) 92.
[20] Z. Fu, N. Wang, D. Legut, et al., Rational design of flexible two-dimensional MXenes with multiple functionalities, Chem. Rev. 119 (23) (2019) 11980–12031.
[21] Y. Wu, X. Li, H. Zhao, et al., Recent advances in transition metal carbides and nitrides (MXenes): characteristics, environmental remediation and challenges, Chem. Eng. J. 418 (2021), 129296.
[22] K. Gong, K. Zhou, X. Qian, et al., MXene as emerging nanofillers for high-performance polymer composites: a review, Compos. Part B: Eng. 217 (2021), 108867.
[23] Z. Li, Z. Lin, Self-assembly of bolaamphiphiles into 2D nanosheets via synergistic and meticulous tailoring of multiple noncovalent interactions, ACS Nano 15 (2) (2021) 3152–3160.
[24] M. Yu, S. Zhou, Z. Wang, et al., Boosting electrocatalytic oxygen evolution by synergistically coupling layered double hydroxide with MXene, Nano Energy 44 (2018) 181–190.
[25] C. Zhang, Interfacial assembly of two-dimensional MXenes, J. Energy Chem. 60 (2021) 417–434.
[26] Y. Zheng, B. Cheng, W. You, et al., 3D hierarchical graphene oxide-NiFe LDH composite with enhanced adsorption affinity to Congo red, methyl orange and Cr (VI) ions, J. Hazard. Mater. 369 (2019) 214–225.
[27] Z.-z Yang, C. Zhang, G.-m Zeng, et al., Design and engineering of layered double hydroxide based catalysts for water depollution by advanced oxidation processes: a review, J. Mater. Chem. A 8 (8) (2020) 4141–4173.
[28] Y. Xue, Q. Zhang, W. Wang, et al., Opening two-dimensional materials for energy conversion and storage: a concept, Adv. Energy Mater. 7 (19) (2017), 1602684.
[29] G. Fan, F. Li, D.G. Evans, et al., Catalytic applications of layered double hydroxides: recent advances and perspectives, Chem. Soc. Rev. 43 (20) (2014) 7040–7066.
[30] J. Wang, R. Huang, W. Qi, et al., Preparation of amorphous MOF based biomimetic nanozyme with high laccase- and catecholase-like activity for the degradation and detection of phenolic compounds, Chem. Eng. J. (2022) 434.
[31] X. Qiu, Y. Wang, Y. Xue, et al., Laccase immobilized on magnetic nanoparticles modified by amino-functionalized ionic liquid via dialdehyde starch for phenolic compounds biodegradation, Chem. Eng. J. 391 (2020), 123564.
[32] C. Chen, W. Sun, H. Lv, et al., Spacer arm-facilitated tethering of laccase on magnetic polydopamine nanoparticles for efficient biocatalytic water treatment, Chem. Eng. J. 350 (2018) 949–959.
[33] F. Ran, Y. Zou, Y. Xu, et al., Fe_3O_4@MoS_2@PEI-facilitated enzyme tethering for efficient removal of persistent organic pollutants in water, Chem. Eng. J. 375 (2019), 121947.
[34] C. Ding, J. Liang, Z. Zhou, et al., Photothermal enhanced enzymatic activity of lipase covalently immobilized on functionalized $Ti_3C_2T_X$ nanosheets, Chem. Eng. J. (2019) 378.
[35] Z. Wang, L. Yang, Y. Zhou, et al., NiFe LDH/MXene derivatives interconnected with carbon fabric for flexible electromagnetic wave absorption, ACS Appl. Mater. Interfaces 13 (14) (2021) 16713–16721.
[36] Z. Wei, X. Ma, Y. Zhang, et al., High-efficiency adsorption of phenanthrene by Fe_3O_4-SiO_2-dimethoxydiphenylsilane nanocomposite: Experimental and theoretical study, J. Hazard. Mater. (2022) 422.
[37] J. Chen, Y. Ren, H. Zhang, et al., Ni-Co-Fe layered double hydroxide coated on Ti_3C_2 MXene for high-performance asymmetric supercapacitor, Appl. Surf. Sci. (2021) 562.
[38] Y. Cui, D. Zhang, K. Shen, et al., Biomimetic anchoring of Fe_3O_4 onto Ti_3C_2 MXene for highly efficient removal of organic dyes by Fenton reaction, J. Environ. Chem. Eng. 8 (2020) 5.
[39] E.H. Ramirez-Soria, U. Leon-Silva, T.E. Lara-Ceniceros, et al., Graphene oxide bifunctionalized with NH_2/$NH^{3+}$and their outstanding-performance against corrosion, Appl. Surf. Sci. (2021) 561.
[40] X. Qiu, S. Wang, S. Miao, et al., Co-immobilization of laccase and ABTS onto amino-functionalized ionic liquid-modified magnetic chitosan nanoparticles for pollutants removal, J. Hazard. Mater. (2021) 401.
[41] C. Chao, Y. Zhao, H. Guan, et al., Improved performance of immobilized Laccase on poly(diallyldimethylammonium chloride) functionalized halloysite for 2,4-dichlorophenol degradation, Environ. Eng. Sci. 34 (10) (2017) 762–770.
[42] T.-T. Xia, C.-Z. Liu, J.-H. Hu, et al., Improved performance of immobilized laccase on amine-functioned magnetic Fe_3O_4 nanoparticles modified with polyethylenimine, Chem. Eng. J. 295 (2016) 201–206.
[43] J. Deng, H. Wang, H. Zhan, et al., Catalyzed degradation of polycyclic aromatic hydrocarbons by recoverable magnetic chitosan immobilized laccase from Trametes versicolor, Chemosphere (2022) 301.
[44] X. Gao, C. Wei, H. Qi, et al., Directional immobilization of D-allulose 3-epimerase using SpyTag/SpyCatcher strategy as a robust biocatalyst for synthesizing D-allulose, Food Chem. 401 (2023), 134199-134199.
[45] D.R. Canchi, D. Paschek, A.E. Garcia, Equilibrium study of protein denaturation by urea, J. Am. Chem. Soc. 132 (7) (2010) 2338–2344.
[46] Q. Chen, R. Groote, H. Schoenherr, et al., Probing single enzyme kinetics in real-time, Chem. Soc. Rev. 38 (9) (2009) 2671–2683.
[47] H. Suo, L. Xu, Y. Xue, et al., Ionic liquids-modified cellulose coated magnetic nanoparticles for enzyme immobilization: improvement of catalytic performance, Carbohydr. Polym. (2020) 234.

[48] I. Mateljak, E. Monza, M. Fatima Lucas, et al., Increasing redox potential, redox mediator activity, and stability in a Fungal Laccase by computer-guided mutagenesis and directed evolution, ACS Catal. 9 (5) (2019) 4561–4572.
[49] K. Zhang, W. Yang, Y. Liu, et al., Laccase immobilized on chitosan-coated Fe_3O_4 nanoparticles as reusable biocatalyst for degradation of chlorophenol, J. Mol. Struct. (2020) 1220.
[50] M.Y. Arica, B. Salih, O. Celikbicak, et al., Immobilization of laccase on the fibrous polymer-grafted film and study of textile dye degradation by MALDI-ToF-MS, Chem. Eng. Res. Des. 128 (2017) 107–119.
[51] G. Bayramoglu, B. Karagoz, M.Y. Arica, Cyclic-carbonate functionalized polymer brushes on polymeric microspheres: immobilized laccase for degradation of endocrine disturbing compounds, J. Ind. Eng. Chem. 60 (2018) 407–417.
[52] G. Bayramoglu, M.Y. Arica, Biodegradation of methylene blue and carbaryl by Trametes versicolor laccase preparations in the presence of a mediator compound, J. Macromol. Sci. Part A: Pure Appl. Chem. 56 (3) (2019) 277–285.
[53] G. Bayramoglu, B. Salih, A. Akbulut, et al., Biodegradation of Cibacron Blue 3GA by insolubilized laccase and identification of enzymatic byproduct using MALDI-ToF-MS: toxicity assessment studies by Daphnia magna and Chlorella vulgaris, Ecotoxicol. Environ. Saf. 170 (2019) 453–460.
[54] X. Lou, F. Zhi, X. Sun, et al., Construction of co-immobilized laccase and mediator based on MOFs membrane for enhancing organic pollutants removal, Chem. Eng. J. (2023) 451.
[55] J. Jia, P. Xue, L. Ma, et al., A novel approach to efficient degradation of pesticide intermediate 2,4,5-trichlorophenol by co-immobilized laccase-acetosyringone biocatalyst, Biochem. Eng. J. (2022) 187.